ANTICANCER RESEARCH *39*: 2415-2427 (2019)
doi:10.21873/anticanres.13359

Synthesis of ^{68}Ga-Labeled Biopolymer-based Nanoparticle Imaging Agents for Positron-emission Tomography

ZOLTÁN KÖRHEGYI[1], DÁVID RÓZSA[1], ISTVÁN HAJDU[2], MAGDOLNA BODNÁR[1], ISTVÁN KERTÉSZ[2], KRISZTINA KEREKES[1], SÁNDOR KUN[1], JÓZSEF KOLLÁR[2], JÓZSEF VARGA[2], ILDIKÓ GARAI[2,3], GYÖRGY TRENCSÉNYI[2,3] and JÁNOS BORBÉLY[4,5]

[1]*BBS Nanotechnology, Debrecen, Hungary;*
[2]*Department of Medical Imaging, Division of Nuclear Medicine and Translational Imaging, Faculty of Medicine, University of Debrecen, Debrecen, Hungary;*
[3]*Scanomed Ltd, Debrecen, Hungary;*
[4]*University of Debrecen, Doctoral School of Clinical Medicine, Debrecen, Hungary;*
[5]*BBS Dominus LLC, Debrecen, Hungary*

Abstract. *Aim: The purpose of this study was to develop a folate receptor-targeted ^{68}Ga-labeled agent for the detection of cancer cells in mouse models of ovarian cancer by dual positron-emission tomography (PET) and magnetic resonance imaging (MRI). Moreover, we aimed to develop a controlled biopolymer-based chemistry that enables linking metal-binding (here Ga-68) chelators. Materials and Methods: The nanoparticle (NP) agent was created by self-assembling of folic acid-modified polyglutamic acid and chelator-modified chitosan followed by radiolabeling with ^{68}Ga (III) ions (^{68}Ga-NODAGA-FA). The structure of modified biopolymers was characterized by spectroscopy. Particle size and mobility were determined. Results: Significant selective binding of NPs was established in vitro using folate receptor-positive KB and -negative MDA-MB-231 cell lines. In vivo tumor uptake of folate-targeted $^{68}Ga^{3+}$-radiolabeled NPs was tested using subcutaneous tumor-bearing CB17 SCID mice models. PET/MR dual modalities showed high tumor uptake with 6.5 tumor-to-muscle ratio and NP localization. Conclusion: In vivo results supporting the preliminary in vitro tests demonstrated considerably higher ^{68}Ga-NODAGA-FA nanoparticle accumulation in KB tumors than in MDA-MB-231 tumors, thereby confirming the folate receptor-mediated uptake of this novel potential PET imaging agent.*

Nanotechnology and its medical application as nanomedicine have been developed over the past decades to produce a new generation of diagnostic, therapeutic and theranostic agents (1, 2). Nanoparticle systems have been investigated and improved as promising candidates for revolution of diagnosis or therapy (3, 4).

In parallel with the development of nanotechnology, increasing interest in molecular imaging supported by nanotechnology (5), to increase the specificity and sensitivity of medical imaging by application of multiple modalities, has emerged (6-8). Several molecular imaging tools are currently available, including ultrasound (US), magnetic resonance imaging (MRI), computed tomography (CT), single-photon-emission computed tomography (SPECT), and positron-emission tomography (PET), and their anatomical and functional combinations such as PET/MRI and SPECT/CT. Increasing research and development is helping overcome the limitations of these techniques. Molecular imaging using nanoparticles has several advantages such as higher sensitivity due to concentrated targeted imaging agents or multimodality due to different transported imaging agents (5).

Nanoparticle formulations made of biodegradable and biocompatible biopolymers with targeting moieties provide an efficient platform to carry diagnostic or therapeutic agents to tumors (9, 10). Demonstrated advantages of polymeric nanoparticles include protection of encapsulated materials against degradation, prolonged biological half-life, specific accumulation in tumors, and efficient cellular internalization (11-13).

Polyelectrolyte polymers can form nanosystems *via* ionic interaction between their oppositely charged functional groups. Due to their capacity for self-assembly, these polyelectrolyte complexes have opened up many new opportunities by producing several types of 3D formulations, such as particles (14), layers (15), and hydrogels (16).

Many attempts have been made to create effective biopolymer-based polyelectrolyte complex nanosystems for

Correspondence to: János Borbély, BBS Dominus LLC, Kiserdő u. 4, Debrecen 4225, Hungary. E-mail: jborbely@med.unideb.hu

Key Words: Poly-gamma-glutamic acid, chitosan, self-assembling nanoparticles, ^{68}Ga-NODAGA, xenograft model.

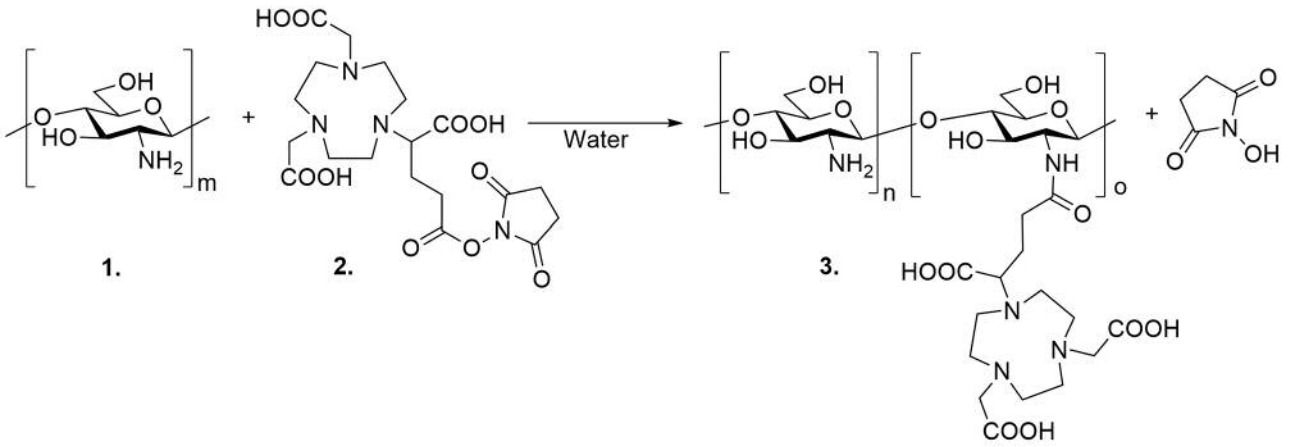

Figure 1. *Schematic representation of the synthesis of modified polymer **3** coupling chitosan **1** and ester **2** resulting in **3**.*

several biomedical applications (17), especially for drug delivery (18, 19). Several research works describe chitosan-based polyelectrolyte complexes (20, 21) and their application possibilities principally as drug delivery systems (22, 23).

Self-assembling nanoparticles of chitosan and poly-γ-glutamic acid (PGA) have been widely investigated as nanostructures (24, 25) and as carriers of poorly water-soluble compounds (26), genes (24), protein (27) or other agents (28).

Our research group has many years of experience and professional success in the field of development of self-assembling nanoparticles, especially from chitosan and PGA, produced as targeted nanosystems (29, 30), or as carriers of potential imaging agents for molecular imaging (31). Chitosan is a renewable biomaterial, β-[1-4]-2-amino-2-deoxy-D-glucopyranose, an amino-functional and basic linear polysaccharide. PGA is an anionic peptide consisting of repetitive glutamic acid units connected by amide linkages between α-amino and γ-carboxylic acid functional groups. Chitosan/PGA self-assembling nanoparticles can form stable complexes with MR active Gd^{3+} ligand (32) or ^{99m}Tc radionuclide (33, 34) and are therefore promising nanocarriers for diagnostic imaging agents.

The present investigation reports the synthesis, characterization, and *in vitro* and *in vivo* study of a novel receptor-targeted PET imaging agent made of chitosan and PGA, biopolymers by self-assembly. The ^{68}Ga-labeled nanoparticles were fully characterized, *in vitro* uptake and cytotoxicity were studied, while biodistribution, and tumor accumulation of this radiotracer were monitored using PET/MRI in *in vivo* experiments.

Materials and Methods

Chemicals. Chitosan **1** (CHI) with degree of acetylation ≤40 mol% and M_v=60-120 kDa, (purchased from Sigma–Aldrich Co., Budapest, Hungary) was dissolved in 2.0% aqueous acetic acid solution, filtered and dialyzed against distilled water until the pH became neutral, then dried by lyophilization.

Poly-gamma-glutamic acid **7** (PGA; M_w=60-120kDa; Shandong Freda Biotechnology Co., Ltd., China) was dissolved in water (1.0% w/w), filtered and dialyzed against distilled water, then dried by lyophilization.

2,2'-(7-(1-Carboxy-4-((2,5-dioxopyrrolidin-1-yl)oxy)-4-oxobutyl)-1,4,7-triazonane-1,4-diyl)diacetic acid (NODAGA) *N l*-hydroxysuccinimide (NHS) ester **2** was purchased from CheMatech (Dijon, France). Anti-folate-binding protein antibody (LK26) was obtained from Abcam, Cambridge, UK. 1-[3-(Dimethylamino) propyl]-3-ethylcarbodiimide hydrochloride (EDC), NHS, 3-[2-(2-(3-(boc-amino)propyloxy)ethoxy)ethoxy]propylamine (PEG amine), folic acid **5** (FA) dehydrate, 1-hydroxybenzotriazole hydrate (HOBt), triethylamine (TEA) as well as all reagents and all solvents – with the exception of solvents for radiolabeling – were purchased from Sigma–Aldrich Co., Budapest, Hungary. They were of analytical grade and were used as received.

*Coupling of chitosan **1** and NODAGA-NHS **2**, synthesis of chitosan derivative **3***. Chitosan **1** (10 mg) was solubilized in 20 ml water; its dissolution was facilitated by dropwise addition of 0.1 M HCl solution. After dissolution, the pH of chitosan solution was adjusted to 6.1. NODAGA-NHS ester **2** was dissolved in dimethyl sulfoxide to produce a solution at a concentration of 10 mg/ml. The NODAGA-NHS solution (460 μl, 10 mg/ml) was added dropwise to chitosan solution and the reaction mixture was stirred at room temperature for 24 h. The chitosan-NODAGA **3** conjugate (CHI-NODAGA) was purified by dialysis (Figure 1). The modification average rate value was 3-7%, and monomer units *n* and *o* ratio value of *n*+*o*/*o*=15 to 34. The number of **2** molecules on the backbone of **1** addresses a statistical random distribution of modified polymer **3**.

*Coupling of PGA **7** and FA **5** via PEG **4**, synthesis of PGA derivative **8***. Synthesis of folate-labeled PGA was performed using a two-step process. Firstly, FA **5** was activated with *N*-hydroxysuccinimide to **5a**, then it was coupled to PEG amine 4 using a reaction described elsewhere (35). Compound **6** was identified by ^1H nuclear magnetic resonance (NMR) spectroscopy. The recorded spectrum was in good agreement with recently published data (36). After that, FA-PEG

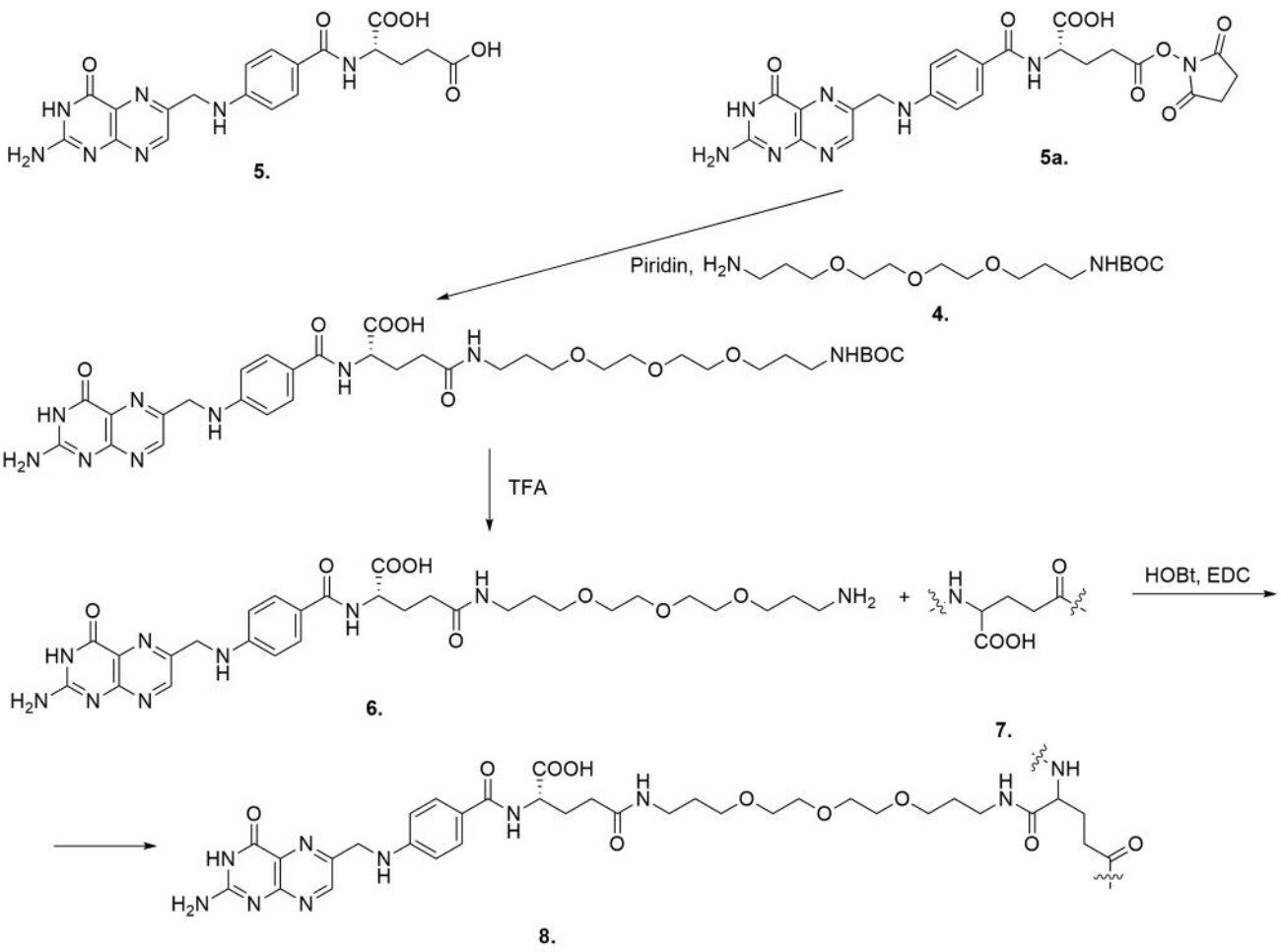

Figure 2. *Schematic representation of the synthesis of* ***8***.

amine **6** was conjugated *via* amino groups to PGA using carbodiimide technique.

Secondly, 300 mg PGA **7** was dissolved in 300 ml water and 94 mg HOBt was added to the solution. The mixture was cooled to 4˚C. Cold EDC solution (445 mg in 15 ml distilled water) was added dropwise to the PGA **7** aqueous solution, and the resulted reaction mixture was stirred at 4˚C for 15 minutes. In the next step, FA-PEG amine **6** (m=100 mg in 15 ml water) was added and the solution was stirred at room temperature for 24 hours. PGA-PEG-FA **8** was purified by dialysis (Figure 2). The ratio of modification on average was 5-7% in respect of the PEG-FA moieties.

Formation of self-assembling nanoparticles ***9***. Stable self-assembling nanoparticles were produced *via* an ionotropic gelation process between PGA-PEG-FA **8** and CHI-NODAGA **3** conjugate. The CHI-NODAGA solution (0.3 mg/ml, 1 ml, pH 4.0) was added into 1 ml of 0.3 mg/ml PGA-PEG-FA solution (pH 9.0) under continuous stirring at room temperature to give an aqueous solution of (37) conjugate nanoparticles **9** (Figure 3). Nanoparticles remained stable at room temperature in solution at physiological pH for several weeks.

Radiolabeling of self-assembling nanoparticles. Radiolabeling was performed based on the general methodology for ^{68}Ga-labeling (38). Briefly, a ^{68}Ge/^{68}Ga generator (Obninsk, Eckert & Ziegler, Germany) was eluted with 0.1 M HCl (Ultrapur®), (Merck Millipore, Budapest, Hungary). The 1 ml fraction with the highest activity (280±20 MBq) was buffered with 150 µl sodium acetate buffer solution (1 M; Ultrapur®water) and 60 µl of 2% w/w NaOH to adjust the pH to 4.5. Thereafter, a 1.290 ml aqueous solution of 0.3 mg/ml NODAGA nanoparticles was added to the buffered eluent. The mixture was incubated at room temperature for 15 minutes. The raw product (^{68}Ga-NODAGA-nanoparticle) was purified using a Sephadex™ G-25M PD-10 column (Sartorius Stedim Hungaria Ltd., Budakeszi, Hungary) and sterile filtered using a sterile syringe filter with a 0.22 µm pore size. Osmolarity was adjusted to 280±10 mOsm/l with 5% glucose solution (Figure 3).

Characterization of biopolymers and nanoparticles. Hydrodynamic size and size distribution of particles were measured using a dynamic light scattering (DLS) technique with a Zetasizer Nano ZS (Malvern Panalytical Ltd., Malvern, UK). This system was equipped with a 4

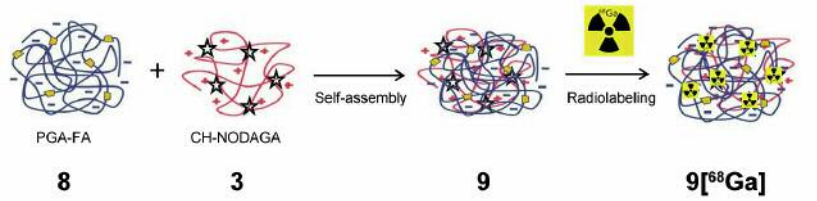

Figure 3. *Schematic drawing of preparation of nanoparticles **9** and subsequent radiolabeling procedures of radiolabeled nanoparticles **9[^{68}Ga]**.*

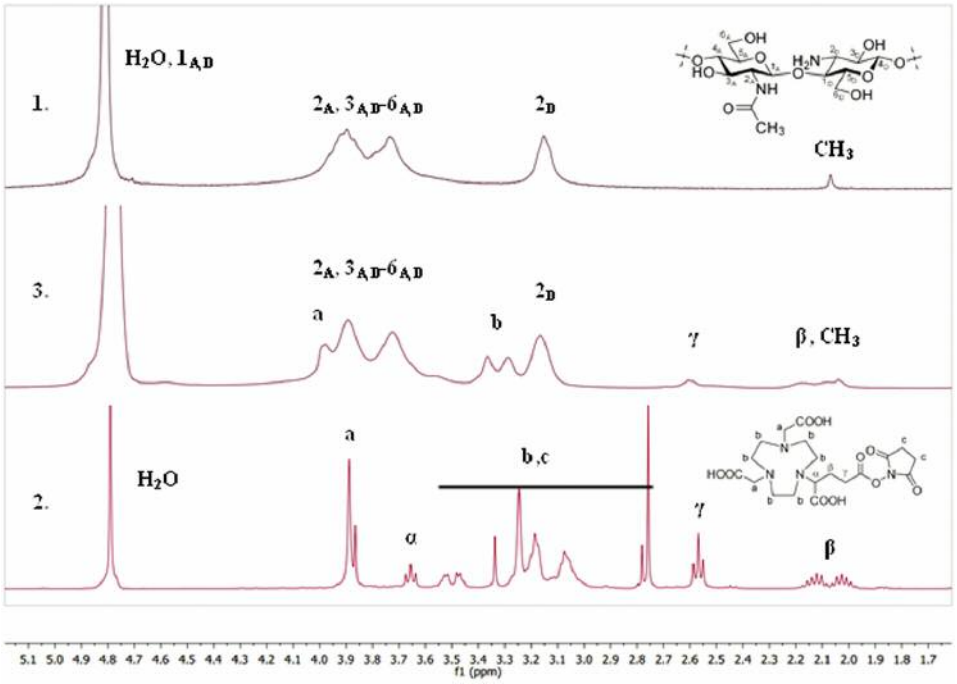

Figure 4. *Comparison of spectra of the biopolymer chitosan (CHI) **1** and CHI-conjugated with 2,2'-(7-(1-carboxy-4-((2,5-dioxopyrrolidin-1-yl)oxy)-4-oxobutyl)-1,4,7-triazonane-1,4-diyl)diacetic acid (NODAGA) chelator **3**.*

mW 633 nm helium/neon laser and measured the particle size with back scattering at a detection angle of 173˚. Each sample was measured three times, and the average values were calculated. UV spectra of PGA-FA conjugate were measured using a Hitachi U-1900 spectrophotometer (Auro-Science Consulting Ltd., Budapest, Hungary). Gel permeation chromatography analysis was carried out with a Waters e2695 Separations Module (Waters Co., Milford, MA, USA) using an Ultrahydrogel Linear column (Waters, 7.8×300 mm, 10 μm) equipped with a UV/Vis detector (Waters 2489 UV/Vis detector). ^{1}H-NMR spectroscopy measurements were carried out on a Bruker 400 MHz instrument (Flextra Lab Ltd., Budapest, Hungary) in D_2O.

Characterization of radiolabeled ^{68}Ga-NODAGA nanoparticles. Radiochemical purity (RCP) was examined by means of thin layer chromatography (TLC), using TLC silica gel 60 (Merck). Plates were developed in 0.1 M Na-citrate (Rf=0.0 for the labeled nanoparticles and Rf=1.0 for the free metal ions). Radioactivity values on the developed TLC plates were measured by radio TLC scanner (MiniGita, Raytest, Elysia S.A., Angleur, Belgium). RCP% was obtained by manual integration and comparison of the values of the detected activity distribution was provided by using GINA Star TLC™ v.2.18 (Raytest) software.

In order to test the stability of the ^{68}Ga-NODAGA-nanoparticle in mouse serum, 50 μl radiotracer solution was incubated at 37˚C in 500 μl normal mouse serum (BALB/c).

In vitro and in vivo studies

Cancer cell lines. Folate receptor-positive KB human cervical carcinoma cell line, and folate receptor-negative MDA-MB-231 human breast adenocarcinoma cells were selected in order to compare the activity on targeted and non-targeted cells. Both cell lines were purchased from Cell Lines Service GmbH, Eppelheim, Germany. Cells were grown as monolayer cultures in a 5% (v/v) CO_2 humidified atmosphere at 37˚C and passaged in Dulbecco's modified Eagle's medium supplemented with 10% fetal calf serum (Invitrogen Life Technologies, Carlsbad, CA, USA). The examined cells were maintained in FA-free RPMI supplemented with 10% fetal calf serum for 2 days before the experiments.

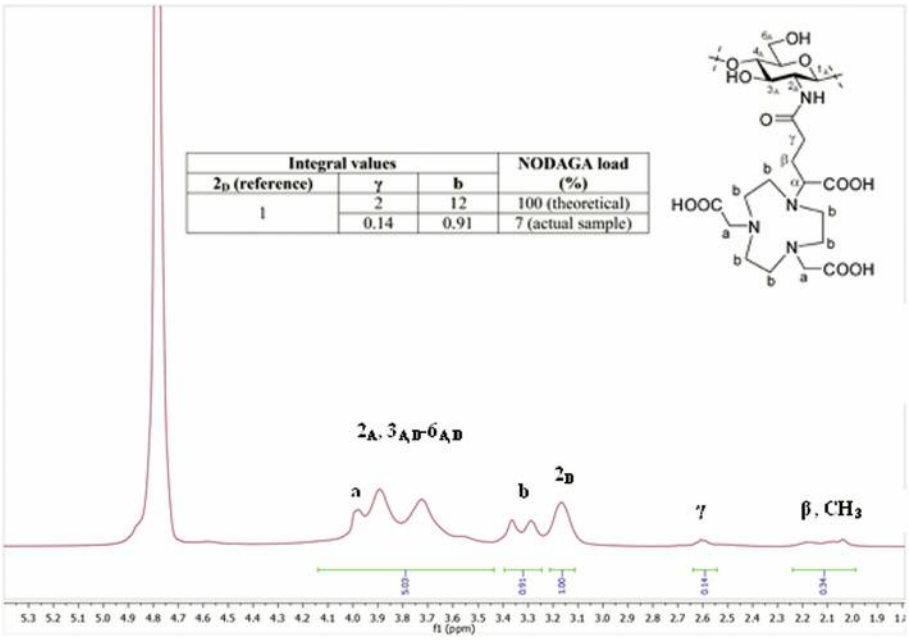

Figure 5. *[1]H-Nuclear magnetic resonance spectrum of **3** chitosan–2,2'-(7-(1-carboxy-4-((2,5-dioxopyrrolidin-1-yl)oxy)-4-oxobutyl)-1,4,7-triazonane-1,4-diyl)diacetic acid (CHI-NODAGA).*

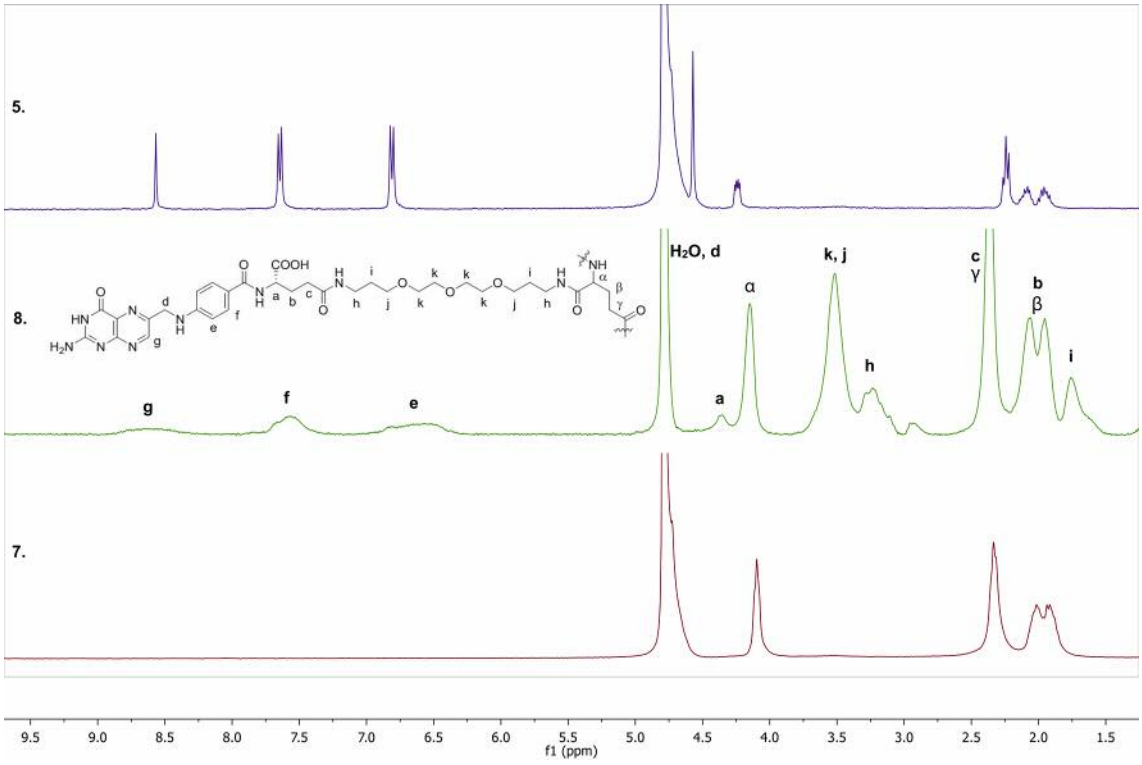

Figure 6. *Structure of poly-gamma-glutamic acid (PGA) **7** conjugated with folic acid **5** through 3-[2-(2-(3-(boc-amino)propyloxy)ethoxy)ethoxy]propylamine (PEG amine) **4** linker.*

Laboratory animals. Laboratory animals were kept and treated in compliance with all applicable sections of the Hungarian Laws and animal welfare directions and regulations of the European Union. The Governmental Ethical Committee approved the study (permission no. 22. 1/609/001/2010). The experimental protocol was approved by the Laboratory Animal Care and Use Committee of the University of Debrecen.

The experiments were carried out using immunocompromised CB17 female SCID mice (n=12) (Laboratory Animal Core Facility, University of Debrecen, Debrecen, Hungary). The diet and drinking water (sterilized by autoclaving) were available ad libitum to all the animals.

Animal model and study design. KB and MDA-MB-231 tumor xenografts were induced by subcutaneous injection of 3×10^6 cells in 150 μl sterile filtered physiological saline into the femoral region of mice. PET/MRI and *ex vivo* biodistribution experiments were carried out 10±2 days after tumor cell implantation.

PET/MRI using ^{68}Ga-NODAGA nanoparticles. Tumor-bearing mice were injected with 7.4±0.3 MBq of ^{68}Ga-NODAGA nanoparticles *via* the lateral tail vein in 0.15 ml volume. At 90 minutes after the injection, animals were anesthetized by 3% isoflurane with a dedicated small animal anesthesia device and whole-body PET scans (20-minutes static PET scans) were acquired using a preclinical nanoScan PET/MRI system (Mediso Ltd., Budapest, Hungary)

Radiotracer uptake was expressed in terms of the standardized uptake value (SUV). Ellipsoidal 3-dimensional volumes of interest (VOI) were manually drawn around the edge of the tissue or organ activity by visual inspection using InterView™ FUSION multi-modal visualization and evaluation software (Mediso Ltd.). The SUV was calculated as follows: SUV=[VOI activity (Bq/ml)]/[injected activity (Bq)/animal weight (g)], assuming a density of 1 g/ml.

Ex vivo biodistribution study. Experimental animals (n=3) were anaesthetized and injected with 7.4±0.3 MBq ^{68}Ga-NODAGA nanoparticles *i.v.* in saline. After 90 minutes incubation, mice were euthanized with isoflurane (3%) and blood samples were taken from the aorta. Tissue samples were taken from each organ and their specific activities were measured with a gamma counter (Packard Cobra II; Canberra Packard Ltd., Budapest, Hungary). The weight and the radioactivity of the samples were used to determine the differential absorption ratio (DAR).

DAR was calculated as:

$$\text{DAR} = \frac{\text{(accumulated radioactivity/g tissue)}}{\text{(total injected radioactivity/body weight)}}$$

Statistical analysis. Data are presented as mean±SD of at least three independent experiments. Statistical significance was calculated by Student's *t*-test (two-tailed) using GraphPad Prism version 5.00 for Windows (GraphPad Software, La Jolla, CA, USA) Level of significance was set at $p\leq0.05$ unless otherwise indicated.

Results

*Synthesis and structural determination of modified polymers **3** and **8***. Structures of conjugated polymers were demonstrated by 1H-NMR spectroscopy. ^{1}H-NMR spectra of CHI, NODAGA-NHS ester **2** and that of the conjugated polymer **3** (CHI-NODAGA) are shown in Figure 4. The signal assignment is based on a published and fully assigned spectrum of a NODAGA tBu-ester derivative (39). The significant β and γ protons originating from NODAGA appear in the conjugated polymer spectrum at 2.6 ppm and 1.9-2.2 ppm, respectively. ^{1}H-NMR spectrum of **3** (CHI-NODAGA) is shown in Figure 5. NODAGA load was calculated from the integral values of 2_D, b and γ, since these peaks can be identified easily and only slightly overlap. The modification rate value was 7%, and monomer units *n* and *o* ratio value of $n+o/o=15$.

The new polymer PGA-PEG-FA **8** consists of three elements: PGA polymer **7**, PEG oligomer **4**, and folic acid **5**, and it was synthesized as shown in Figure 2.

^{1}H-NMR spectra of **7**, **5** raw materials and the modified polymer **8** are shown in Figure 6, and the assignments are inserted. The h, i, j and k protons of the PEG oligomer **4** are assigned in the spectrum of **8** modified polymer. The e, f and g aromatic protons of FA 5 are broader, due to their relaxation time in the polymeric environment in **8**.

Typical protons in the new polymer are: a (4.12 ppm) and α (4.05 ppm) originate from FA **5** and PGA **7**, respectively. Typical protons of PEG **4** residue in the new polymer are in the range of 3.50 ppm (k and j), 3.20 (h) and 1.41 ppm (i). The protons β,β' and γ of PGA overlap with protons b and c of FA (range=1.75-2.40 ppm). However, protons g, f, and e indicate the presence of FA in the new polymer PGA-PEG-FA **8**.

Formation and characterization of nanoparticles. Nanoparticles were prepared from the modified PGA **8** and chitosan **3** biopolymers. The size exclusion chromatogram shows a single peak that proves the homogeneity of nanoparticles **9** (Figure 7A). The hydrodynamic size of the self-assembling nanoparticles was 110±10 nm, with monomodal size distribution between 70 and 150 nm (Figure 7B-D). The zeta potential of the nanoparticles was −38.8 mV at pH 7.4 (Figure 7E). Nanoparticles remained stable at room temperature in solution at physiological pH for several weeks (Figure 7F).

Cytotoxicity of NODAGA nanoparticles. The viability of KB and MDA-MB-231 cells treated with NODAGA nanoparticles was investigated using an MTT assay. The viability of KB cells treated with NODAGA nanoparticles after 72 h was 91±1.8%. The viability of MDA-MB-231 cells treated with NODAGA nanoparticles after 72 h was 89±1.3%. Viability of KB cells without treatment was used as a control set at 100%

The MTT assay indicated no significant change in cell viability at 30 μg/ml nanoparticle concentration, which was used in the *in vivo* experiments.

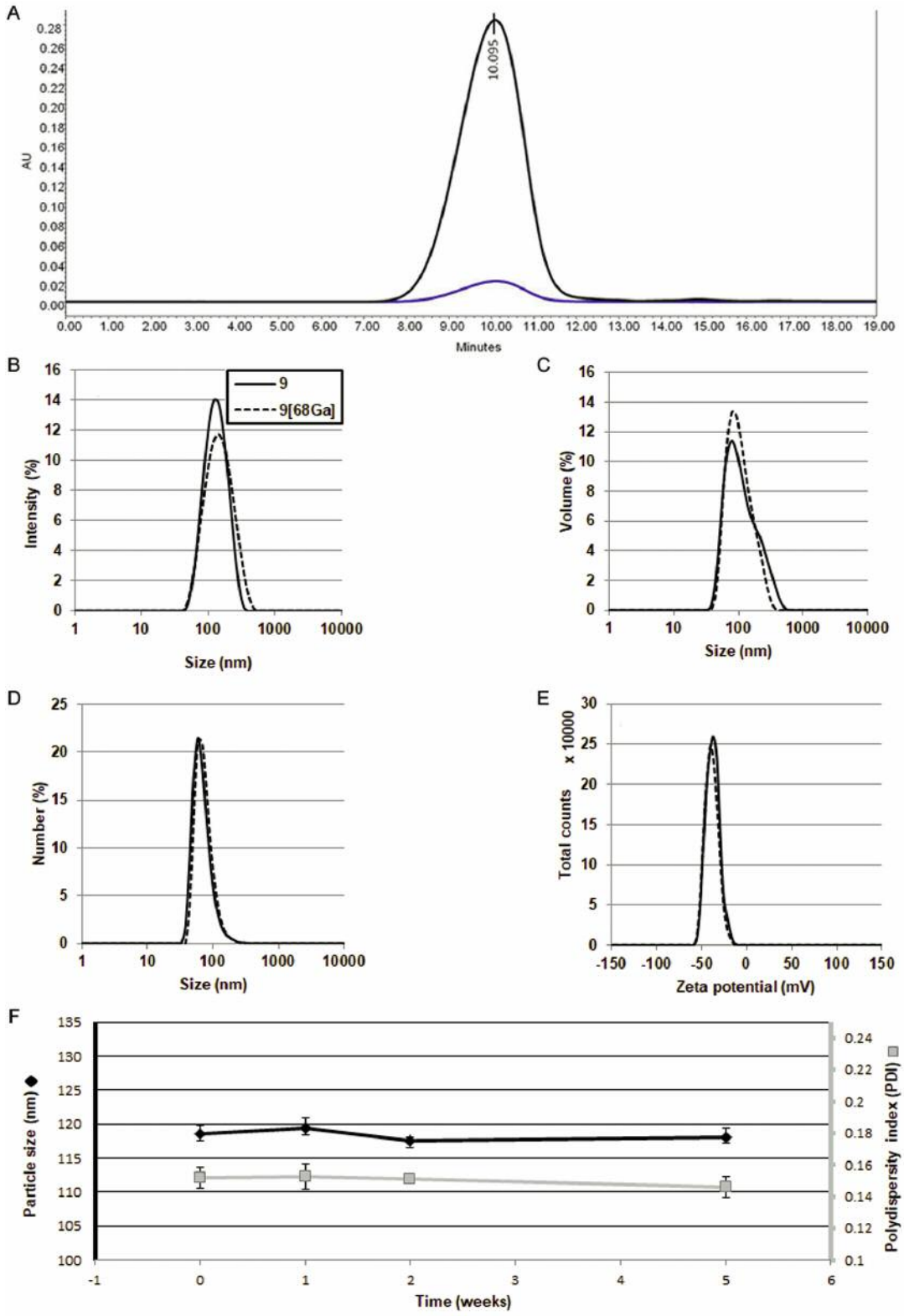

Figure 7. *Chromatogram of 2,2'-(7-(1-carboxy-4-((2,5-dioxopyrrolidin-1-yl)oxy)-4-oxobutyl)-1,4,7-triazonane-1,4-diyl)diacetic acid (NODAGA) nanoparticles* ***9*** *displayed one monomodal fraction at 10.095 min, indicating only one kind of nanoparticle. A: The NODAGA nanoparticles* ***9*** *and the* ^{68}*Ga-NODAGA nanoparticles* ***9[^{68}Ga]*** *had narrow hydrodynamic size distribution in intensity (B), volume (C), number (D) mode and the zeta potential (E). F: Storage stability of NODAGA nanoparticles. Size and polydispersity index of nanoparticles were recorded for 5 weeks.*

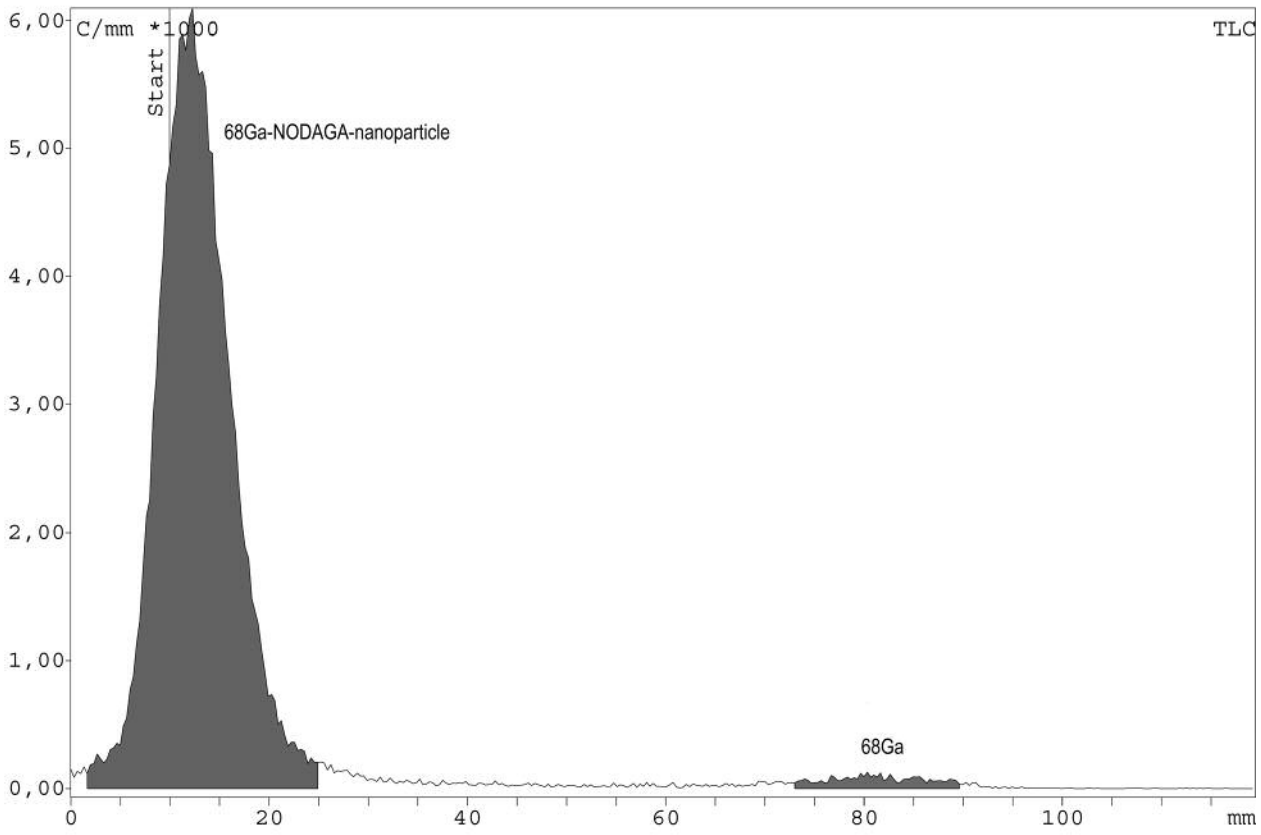

Figure 8. *Representative radio-thin layer chromatogram of ^{68}Ga-labeled nanoparticles before gel filtration.*

Expression of folate receptors. Folate receptors were detected using LK26 α-FR-specific monoclonal mouse antibody. As the flow cytometric data demonstrate, KB cells express a large number of folate receptors on their surface, and these cells are considered to be folate receptor-positive (40). MDA-MB-231 cells contain only a few receptors on their surface and therefore are considered to be folate receptor-negative. The functional analysis showed high uptake of the fluorescent FA analog in the case of the KB cells, which was competed off with an excess amount of natural FA. The uptake of the MDA-MB-231 cells was low and the addition of FA did not affect the measured fluorescence.

*The radiolabeling efficiency of ^{68}Ga-NODAGA nanoparticles **9[Ga-68]***. The radiolabeling efficiency of ^{68}Ga-NODAGA nanoparticles was found to be more than 94% (Figure 8). Radiochemical purity of the ^{68}Ga-NODAGA nanoparticles after gel-filtration was found to be 98.2±1%. The maximum specific radioactivity value of **9[Ga-68]** was 0.775 GBq/mg.

After a 3-hour incubation of **9[Ga-68]** at room temperature in mouse serum, the initial RCP% did not change. In all experiments >95% radiochemical purity was observed indicating that no release or serum protein-assisted decomplexation of the radiolabel occurs under physiological conditions within the time-frame of the *in vivo* experiments.

In vitro radiotracer uptake studies. Folate receptor-positive KB and receptor-negative MDA-MB-231 cell lines were compared in the *in vitro* ^{68}Ga-NODAGA-FA nanoparticle **9[Ga-68]** uptake studies (Figure 9A).

The radiotracer uptake of KB cells overexpressing the folate receptor was found to be four-times higher than that of the control MDA-MB-231 cells after 30 minutes of incubation. Only moderate increase was observed at later time points (up to 4.5-fold maximal uptake). At each time point, significant differences ($p<0.05$) were observed between the folate receptor-positive and control cell lines. Co-incubation with 1 mM folic acid significantly reduced the uptake of the KB cells ($p<0.05$), but it did not affect the observed uptake by MDA-MB-231 cells (Figure 9B).

Ex vivo biodistribution studies on KB xenograft tumors. Tumor-bearing mice were injected with ^{68}Ga-NODAGA-nanoparticle intravenously 10±2 days after KB tumor cell

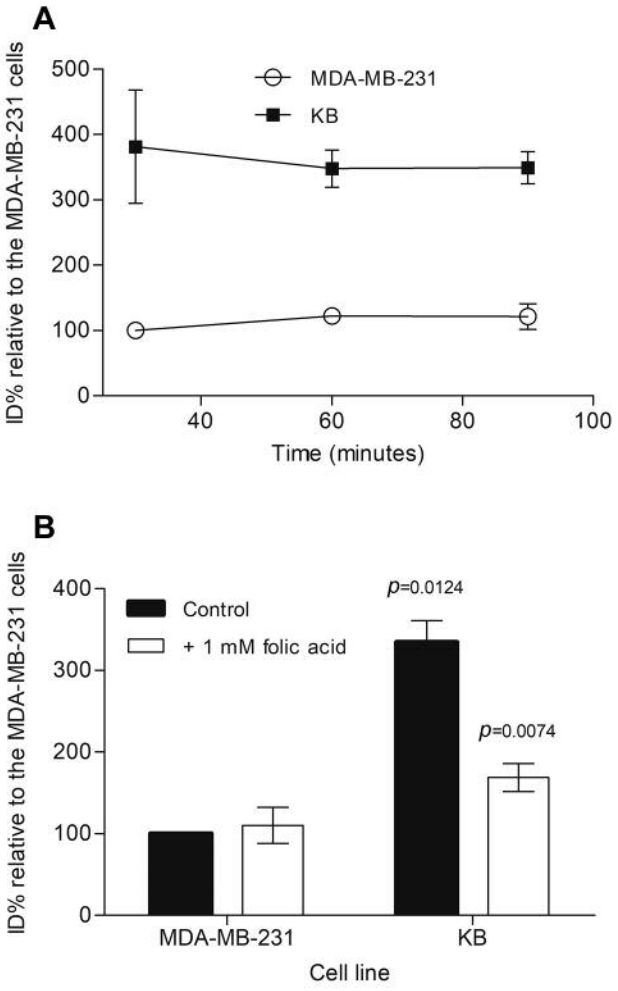

Figure 9. *A: Cellular uptake of the ^{68}Ga-labeled nanoparticles at different time points. B: Cellular uptake of ^{68}Ga-labeled nanoparticles at 60 min. Uptake is expressed as a percentage of the contrast agent uptake of MDA-MB-231 cells in the earliest (30 min) measurement. KB cells displayed a significantly higher uptake, but addition of folic acid reduced the uptake. Values are means±S.D. of three independent experiments.*

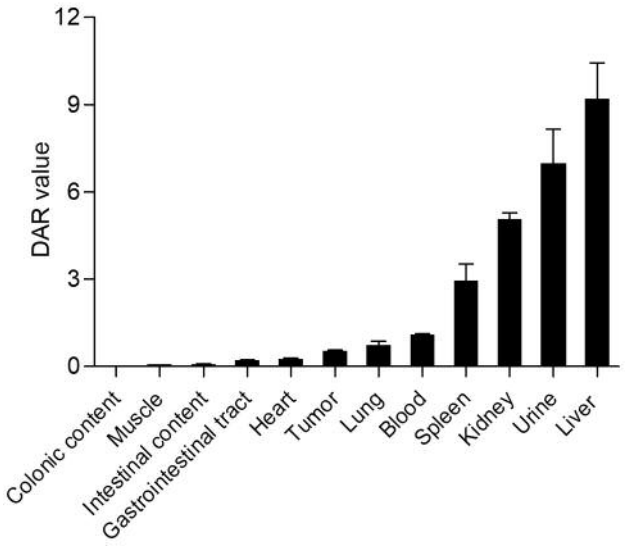

Figure 10. *Biodistribution of the ^{68}Ga-labelled nanoparticles 90 minutes after their injection intravenously in mice bearing KB tumors. The uptake values are presented as means±S.D differential absorption ratio (DAR) values of three independent experiments. The non-specific uptake of the liver and the spleen was high, and the kidney also showed nanoparticle accumulation. The tumor to muscle tissue uptake ratio of the accumulated radioactivity in KB was 6.10±0.60.*

inoculation. Mice were sacrificed 90 minutes after tracer injection and *ex vivo* biodistribution studies were performed (Figure 10). For the quantitative analysis of the uptake by different organs, DAR values were calculated. At 90 minutes after the ^{68}Ga-NODAGA-nanoparticle injection, uptake in the liver and kidneys was relatively high (DAR values were 9.21±2.12 and 5.07±0.36, respectively). The gastrointestinal tract (0.21±0.01), muscle (0.08±0.001), lung (0.74±0.17), spleen (2.96±0.97), and blood (1.09±0.06) showed moderate uptake. By taking the ratio of the DAR values of KB tumor xenograft and muscle (T/M ratio), we found that the DAR value of the tumor was ~6-times higher (tumor/muscle ratio: 6.54±0.6) than that of the muscle.

PET/MRI of tumor xenografts. In vivo PET/MRI experiments were carried out 10±2 days after KB and MDA-MB-231 tumor cell implantation (Figure 11). MRI provides three-dimensional anatomic images in a noninvasive way with excellent spatial and contrast resolution, allowing tumor evaluation.

However, molecular changes (including folate surface receptors), which normally precede morphological alterations, are not recognized by any of the traditional techniques (Figure 11) and their detection requires functional imaging of characteristic cell receptors.

Fusion of T1-weighted MRI and ^{68}Ga PET images depict both anatomical structures and the locations of the targeted tracer, *i.e.* location of the FA receptors on the surface of cancer cells.

Combined analysis of anatomical and molecular findings allows for a more comprehensive assessment of the extent of a neoplastic disease.

The folate receptor positive KB tumor xenografts were clearly visualized by using folate targeted ^{68}Ga-NODAGA-nanoparticle after 90 minutes. In contrast, folate receptor-negative MDA-MB-231 tumors were seen only on MRI images. After quantitative analysis of PET images, SUVmean and SUVmax values of the KB tumors were found to be 0.32±0.17 and 1.75±2.13, respectively. These SUV values were approximately two times higher than that of the MDA-

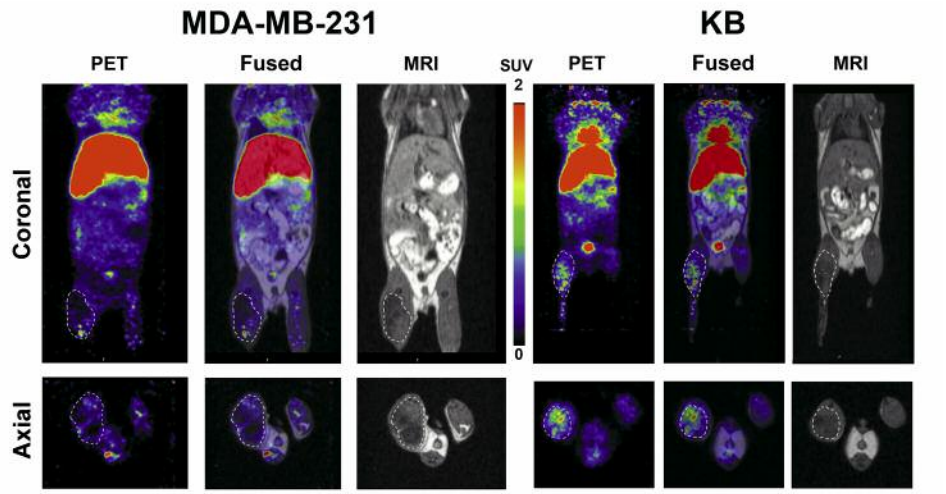

Figure 11. *Whole-body fused mini positron-emission tomography/magnetic resonance imaging (PET/MRI) of the ^{68}Ga-labeled nanoparticles in tumor-bearing mice. PET scans were acquired 90 minutes post injection of nanoparticles. Arrows indicate tumor locations. SUV: Standardized uptake value.*

MB-231 tumors, where the SUVmean and SUVmax values were 0.14±0.03 and 1.03±0.13, respectively. By analyzing T/M ratios, the ^{68}Ga-NODAGA nanoparticle uptake in KB tumors was significantly ($p \leq 0.02$) higher than in MDA-MB-231 tumors.

Discussion

Small animal PET imaging techniques are well established and widely used non-invasive methods in preclinical studies for the detection of tumors, staging, and monitoring the efficacy of therapy (41, 42). Folate receptor is one of the frequent tumor-associated targets for cancer imaging because these receptors are overexpressed on a number of cancer cell lines, but their expression is limited in normal, healthy tissues (43-45), except in wound healing, pregnancy, *etc*.

Biodegradable nanoparticles associated with tumor receptor binding ligands for targeting may have remarkable potential as diagnostic imaging agents in oncology (46). Labeling these targeted nanoparticles with positron-emitting radionuclides is a promising method for contrast agent applications for functional imaging.

In this present study, we investigated a biodegradable folic acid targeted ^{68}Ga-NODAGA nanoparticles as a new PET radiotracer for imaging of folate receptor-positive cells.

The prepared self-assembling nanoparticles were 110±10 nm in size with a narrow size distribution and negative surface charge. The quantitative radiolabeling yield for ^{68}Ga-NODAGA-nanoparticle was more than 95% and the maximum specific radioactivity was 0.775 GBq/mg, therefore the ^{68}Ga-NODAGA nanoparticles were suitable for performing further *in vitro* and *in vivo* investigations.

The folate receptor-positive KB (human carcinoma) and folate receptor-negative MDA-MB-231 (human breast cancer) cell lines were used under *in vitro* and *in vivo* conditions. Significant differences ($p \leq 0.05$) in *in vitro* ^{68}Ga-NODAGA-nanoparticle uptake studies were observed between folate receptor-positive and-negative cell lines over a range of incubation times. These results correlated with our flow cytometric measurements where the expression of receptors was investigated. We found similar results when the internalization of folic acid-targeted Alexa Fluor 488-, Alexa Fluor 546- and Gd-conjugated nanoparticles were investigated with KB and HeDe tumor cells by flow cytometry and fluorescence microscopy (31, 32).

MTT assay showed no significant change in cell viability *in vitro*, suggesting that ^{68}Ga-NODAGA nanoparticles were non-toxic.

For *ex vivo* biodistribution studies, tumor-bearing mice were injected with ^{68}Ga-NODAGA nanoparticles intravenously after 10±2 days after KB tumor cell inoculation. DAR values showed high radiotracer uptake in the liver, kidneys and urine. The reason for the high liver ^{68}Ga-NODAGA-nanoparticle uptake is that the hepatobiliary system of the liver represents the primary route of excretion for particles because of the large phagocytic capacity of Kupffer cells, and the processing pathways of foreign particles of the hepatocytes (46). Longmire *et al*. described that the renal clearance of intravascular agents is considerable, mostly of intravenously injected nanoparticles (46). Furthermore, kidneys may also have high folate receptor expression in the proximal tubules (47). High radiotracer uptake was observed in KB tumors, where the T/M ratio was 6.54±0.6. This value indicates that our ^{68}Ga-NODAGA nanoparticles are applicable for the detection of folate receptor-positive tumors.

For *in vivo* PET imaging studies, xenograft tumors were induced by subcutaneous injection of KB and MDA-MB-231 tumor cells into the right femoral region of the animals. Our aim was to compare the uptake of the ^{68}Ga-NODAGA nanoparticles in folate receptor-positive and -negative tumors using PET/MRI. Evaluation of uptake was based on normalizing the radiotracer uptake tumor tissue to that of muscle tissue, which has a low metabolic rate. A high T/M ratio results in good contrast in preclinical and clinical PET images (48). The 6.54±0.6 T/M ratio of ^{68}Ga-NODAGA nanoparticles provided good quality PET/MRI fusion images.

Our data demonstrate that this new PET tracer is suitable for imaging folate receptor-overexpressing tumor cells.

Conclusion

The high *in vivo* tumor accumulation values and high T/M ratio values demonstrate that ^{68}Ga-NODAGA-FA nanoparticles are promising in tumor diagnostics, and after further successful preclinical studies may be used for functional imaging of folate receptor-overexpressing human cancer.

Conflicts of Interest

The Authors declare no conflict of interest in regard to this study.

Authors' Contributions

Z.K., D.R., I.K., I.H. designed and performed experiments, analyzed data and wrote the article. J.K., M.B. and J.B. were involved in planning and supervised the work. GY.T. and I.G. designed and performed the experiments, derived the models and analyzed the data. J.V., I.G., K.K. and M.B. co-wrote the article in consultation with J.B., I.K. and GY.T. D.R., S.K. and K.K. processed the experimental data, performed the analysis, and designed the figures. S.K. characterized samples with spectroscopy and designed the figures. I.H. and Z.K. manufactured the samples. All Authors discussed the results and commented on the article.

Acknowledgements

This work is supported by JEREMIE-Joint European Resources for Micro to Medium Enterprises.

References

1 Xie J, Lee S and Chen X: Nanoparticle-based theranostic agents. Adv Drug Deliv Rev *62(11)*: 1064-1079, 2010. PMID: 20691229. DOI: 10.1016/j.addr.2010.07.009

2 Janib SM, Moses AS and MacKay JA: Imaging and drug delivery using theranostic nanoparticles. Adv Drug Deliv Rev *62(11)*: 1052-1063, 2010. PMID: 20709124. DOI: 10.1016/j.addr.2010.08.004

3 Mura S and Couvreur P: Nanotheranostics for personalized medicine. Adv Drug Deliv Rev *64(13)*: 1394-1416, 2012. PMID: 22728642. DOI: 10.1016/j.addr.2012.06.006

4 Polyak A and Ross TL: Nanoparticles for spect and pet imaging: Towards personalized medicine and theranostics. Curr Med Chem *25(34)*: 4328-4353, 2018. PMID: 28875837. DOI: 10.2174/0929867324666170830095553

5 Agrawal P, Strijkers GJ and Nicolay K: Chitosan-based systems for molecular imaging. Adv Drug Deliv Rev *62(1)*: 42-58, 2010. PMID: 19861142. DOI: 10.1016/j.addr.2009.09.007

6 Ryu JH, Koo H, Sun IC, Yuk SH, Choi K, Kim K and Kwon IC: Tumor-targeting multi-functional nanoparticles for theragnosis: New paradigm for cancer therapy. Adv Drug Deliv Rev *64(13)*: 1447-1458, 2012. PMID: 22772034. DOI: 10.1016/ j.addr.2012.06.012

7 Zhou Z and Lu ZR: Molecular imaging of the tumor microenvironment. Adv Drug Deliv Rev *113*: 24-48, 2017. PMID: 27497513. DOI: 10.1016/j.addr.2016.07.012

8 Yang X, Hong H, Grailer JJ, Rowland IJ, Javadi A, Hurley SA, Xiao Y, Yang Y, Zhang Y, Nickles RJ, Cai W, Steeber DA and Gong S: Crgd-functionalized, dox-conjugated, and ^{64}Cu-labeled superparamagnetic iron oxide nanoparticles for targeted anticancer drug delivery and PET/MR imaging. Biomaterials *32(17)*: 4151-4160, 2011. PMID: 21367450. DOI: 10.1016/j.biomaterials.2011.02.006

9 Ali A and Ahmed S: A review on chitosan and its nanocomposites in drug delivery. Int J Biol Macromol *109*: 273-286, 2018. PMID: 29248555. DOI: 10.1016/j.ijbiomac.2017.12.078

10 Tabasum S, Noreen A, Kanwal A, Zuber M, Anjum MN and Zia KM: Glycoproteins functionalized natural and synthetic polymers for prospective biomedical applications: A review. Int J Biol Macromol *98*: 748-776, 2017. PMID: 28111295. DOI: 10.1016/j.ijbiomac.2017.01.078

11 Zhang L, Chan JM, Gu FX, Rhee JW, Wang AZ, Radovic-Moreno AF, Alexis F, Langer R and Farokhzad OC: Self-assembled lipid – polymer hybrid nanoparticles: A robust drug delivery platform. ACS Nano *2(8)*: 1696-1702, 2008. PMID: 19206374. DOI: 10.1021/nn800275r

12 Kamaly N, Xiao Z, Valencia PM, Radovic-Moreno AF and Farokhzad OC: Targeted polymeric therapeutic nanoparticles: Design, development and clinical translation. Chem Soc Rev *41(7)*: 2971-3010, 2012. PMID: 22388185. DOI: 10.1039/ c2cs15344k

13 Chou LY, Ming K and Chan WC: Strategies for the intracellular delivery of nanoparticles. Chem Soc Rev *40(1)*: 233-245, 2011. PMID: 20886124. DOI: 10.1039/c0cs00003e

14 Suna Y, Liu Y, Liu W, Lu C and L W: Chitosan microparticles ionically cross-linked with poly (-glutamic acid) as antimicrobial peptides and nitric oxide delivery systems. Biochem Eng J *95*: 78-85, 2015. DOI: 10.1016/j.bej.2014.11.022

15 Antunes JC, Pereira CL, Molinos M, Ferreira-da-Silva F, Dessì M, Gloria A, Ambrosio L, Gonçalves RM and Barbosa MA: Layer-by-layer self-assembly of chitosan and poly (γ-glutamic acid) into polyelectrolyte complexes. Biomacromolecules *12(12)*: 4183-4195, 2011. PMID: 22032302. DOI: 10.1021/bm2008235

16 Chen Y, Yan X, Zhao J, Feng H, Li P, Tong Z, Yang Z, Li S, Yang J and Jin S: Preparation of the chitosan/poly (glutamic acid)/alginate polyelectrolyte complexing hydrogel and study on its drug releasing property. Carbohydr Polym *191*: 8-16, 2018. PMID: 29661325. DOI: 10.1016/j.carbpol.2018.02.065

17 Belluzo MS, Medina LF, Cortizo AM and Cortizo MS: Ultrasonic compatibilization of polyelectrolyte complex based on polysaccharides for biomedical applications. Ultrason Sonochem *30*: 1-8, 2016. PMID: 26703196. DOI: 10.1016/j.ultsonch.2015.11.022

18 Luo Y and Wang Q: Recent development of chitosan-based polyelectrolyte complexes with natural polysaccharides for drug delivery. Int J Biol Macromol *64*: 353-367, 2014. PMID: 24360899. DOI: 10.1016/j.ijbiomac.2013.12.017

19 Bourganis V, Karamanidou T, Kammona O and Kiparissides C: Polyelectrolyte complexes as prospective carriers for the oral delivery of protein therapeutics. Eur J Pharm Biopharm *111*: 44-60, 2017. PMID: 27847276. DOI: 10.1016/j.ejpb.2016.11.005

20 Wasupalli GK and Verma D: Molecular interactions in self-assembled nano-structures of chitosan-sodium alginate based polyelectrolyte complexes. Int J Biol Macromol *114*: 10-17, 2018. PMID: 29551510. DOI: 10.1016/j.ijbiomac.2018.03.075

21 Birch NP and Schiffman JD: Characterization of self-assembled polyelectrolyte complex nanoparticles formed from chitosan and pectin. Langmuir *30(12)*: 3441-3447, 2014. PMID: 24593694. DOI: 10.1021/la500491c

22 Yan JK, Qiu WY, Wang YY, Wu LX and Cheung PCK: Formation and characterization of polyelectrolyte complex synthesized by chitosan and carboxylic curdlan for 5-fluorouracil delivery. Int J Biol Macromol *107(Pt A)*: 397-405, 2018. PMID: 28882758. DOI: 10.1016/j.ijbiomac.2017.09.004

23 Wang F, Yang Y, Ju X, Udenigwe CC and He R: Polyelectrolyte complex nanoparticles from chitosan and acylated rapeseed cruciferin protein for curcumin delivery. J Agric Food Chem *66(11)*: 2685-2693, 2018. PMID: 29451796. DOI: 10.1021/acs.jafc.7b05083

24 Liao ZX, Peng SF, Ho YC, Mi FL, Maiti B and Sung HW: Mechanistic study of transfection of chitosan/DNA complexes coated by anionic poly (γ-glutamic acid). Biomaterials *33(11)*: 3306-3315, 2012. PMID: 22281422. DOI: 10.1016/j.biomaterials.2012.01.013

25 Lin YH, Chung CK, Chen CT, Liang HF, Chen SC and Sung HW: Preparation of nanoparticles composed of chitosan/poly-gamma-glutamic acid and evaluation of their permeability through Caco-2 cells. Biomacromolecules *6(2)*: 1104-1112, 2005. PMID: 15762683. DOI: 10.1021/bm049312a

26 Hong DY, Lee JS and Lee HG: Chitosan/poly-γ-glutamic acid nanoparticles improve the solubility of lutein. Int J Biol Macromol *85*: 9-15, 2016. PMID: 26712702. DOI: 10.1016/j.ijbiomac.2015.12.044

27 Papadimitriou SA, Achilias DS and Bikiaris DN: Chitosan-g-peg nanoparticles ionically crosslinked with poly (glutamic acid) and tripolyphosphate as protein delivery systems. Int J Pharm *430(1-2)*: 318-327, 2012. PMID: 22521711. DOI: 10.1016/j.ijpharm.2012.04.004

28 Liu Y, Sun Y, Xu Y, Feng H, Fu S, Tang J, Liu W, Sun D, Jiang H and Xu S: Preparation and evaluation of lysozyme-loaded nanoparticles coated with poly-γ-glutamic acid and chitosan. Int J Biol Macromol *59*: 201-207, 2013. PMID: 23628585. DOI: 10.1016/j.ijbiomac.2013.04.065

29 Keresztessy Z, Bodnar M, Ber E, Hajdu I, Zhang M, Hartmann JF, Minko T and Borbely J: Self-assembling chitosan/poly-gamma-glutamic acid nanoparticles for targeted drug delivery. Colloid and Polymer Science *287(7)*: 759-765, 2009. DOI: 10.1007/s00396-009-2022-3

30 Hajdu I, Bodnar M, Filipcsei G, Hartmann JF, Daroczi L, Zrinyi M and Borbely J: Nanoparticles prepared by self-assembly of chitosan and poly-gamma-glutamic acid. Colloid Polymer Sci *286(3)*: 343-350, 2008. DOI: 10.1007/s00396-007-1785-7

31 Hajdu I, Trencsenyi G, Bodnar M, Emri M, Banfalvi G, Sikula J, Marian T, Kollar J, Vamosi G and Borbely J: Tumor-specific localization of self-assembled nanoparticle pet/mr modalities. Anticancer Res *34(1A)*: 49-59, 2014. PMID: 24403444

32 Hajdu I, Bodnar M, Trencsenyi G, Marian T, Vamosi G, Kollar J and Borbely J: Cancer cell targeting and imaging with biopolymer-based nanodevices. Int J Pharmaceut *441(1-2)*: 234-241, 2013. PMID: 23246780. DOI: 10.1016/j.ijpharm.2012.11.038

33 Polyák A, Hajdu I, Bodnár M, Trencsényi G, Pöstényi Z, Haász V, Jánoki G, Jánoki GA, Balogh L and Borbély J: (99m)Tc-labelled nanosystem as tumour imaging agent for SPECT and SPECT/CT modalities. Int J Pharm *449(1-2)*: 10-17, 2013. PMID: 23562750. DOI: 10.1016/j.ijpharm.2013.03.049

34 Polyák A, Hajdu I, Bodnár M, Dabasi G, Jóba RP, Borbély J and Balogh L: Folate receptor targeted self-assembled chitosan-based nanoparticles for SPECT/CT imaging: Demonstrating a preclinical proof of concept. Int J Pharm *474(1-2)*: 91-94, 2014. PMID: 25093694. DOI: 10.1016/j.ijpharm.2014.07.055

35 Dhar S, Liu Z, Thomale J, Dai H and Lippard SJ: Targeted single-wall carbon nanotube-mediated Pt (IV) prodrug delivery using folate as a homing device. J Am Chem Soc *130(34)*: 11467-11476, 2008. PMID: 18661990. DOI: 10.1021/ja803036e

36 Frasconi M, Marotta R, Markey L, Flavin K, Spampinato V, Ceccone G, Echegoyen L, Scanlan EM and S G: Multi-functionalized carbon nano-anions as imaging probes for cancer cells. Chemistry *21(52)*: 19071-19080, 2015. PMID: 26577582. DOI: 10.1002/chem.201503166

37 Morales-Avila E, Ferro-Flores G, Ocampo-García BE and Ramírez1 FdM: Radiolabeled nanoparticles for molecular imaging. *In*: Molecular imaging, isbn:978-953-51-0359-2, intech, doi: 105772/31109. Schaller B (ed.). pp. 1-25, 2012.

38 Notni J, Šimeček J, Hermann P and Wester HJ: Trap, a powerful and versatile framework for gallium-68 radiopharmaceuticals. Chemistry *17(52)*: 14718-14722, 2011. PMID: 22147338. DOI: 10.1002/chem.201103503

39 Eisenwiener KP, Prata MI, Buschmann I, Zhang HW, Santos AC, Wenger S, Reubi JC and Mäcke HR: NODAGATOC, a new chelator-coupled somatostatin analogue labeled with [$^{67/68}$Ga] and [^{111}in] for SPECT, PET, and targeted therapeutic applications of somatostatin receptor (HSST2)-expressing tumors. Bioconjug Chem *13(3)*: 530-541, 2002. PMID: 12009943. DOI: 10.1021/ bc010074f

40 Forster MD, Ormerod MG, Agarwal R, Kaye SB and Jackman AL: Flow cytometric method for determining folate receptor expression on ovarian carcinoma cells. Cytometry A *71(11)*: 945-950, 2007. PMID: 17712798. DOI: 10.1002/cyto.a.20456

41 Wester HJ: Nuclear imaging probes: From bench to bedside. Clin Cancer Res *13(12)*: 3470-3481, 2007. PMID: 17575209. DOI: 10.1158/1078-0432.CCR-07-0264

42 Romero E, Martínez A, Oteo M, García A and Morcillo MA: Preparation of ^{68}Ga-labelled dota-peptides using a manual labelling approach for small-animal PET imaging. Appl Radiat Isot *107*: 113-120, 2016. PMID: 26492321. DOI: 10.1016/j.apradiso.2015.10.005

43 Garin-Chesa P, Campbell I, Saigo PE, Lewis JL, Old LJ and Rettig WJ: Trophoblast and ovarian cancer antigen lk26. Sensitivity and specificity in immunopathology and molecular identification as a folate-binding protein. Am J Pathol *142(2)*: 557-567, 1993. PMID: 8434649.

44 Parker N, Turk MJ, Westrick E, Lewis JD, Low PS and Leamon CP: Folate receptor expression in carcinomas and normal tissues determined by a quantitative radioligand binding assay. Anal Biochem *338(2)*: 284-293, 2005. PMID: 15745749. DOI: 10.1016/j.ab.2004.12.026

45 Low PS and Kularatne SA: Folate-targeted therapeutic and imaging agents for cancer. Curr Opin Chem Biol *13(3)*: 256-262, 2009. PMID: 19419901. DOI: 10.1016/j.cbpa.2009.03.022

46 Longmire M, Choyke PL and Kobayashi H: Clearance properties of nano-sized particles and molecules as imaging agents: Considerations and caveats. Nanomedicine *3(5)*: 703-717, 2008. PMID: 18817471. DOI: 10.2217/17435889.3.5.703

47 Müller C: Folate-based radiotracers for PET imaging--update and perspectives. Molecules *18(5)*: 5005-5031, 2013. PMID: 236297 56. DOI: 10.3390/molecules18055005

48 Pollok KE, Lahn M, Enas N, McNulty A, Graff J, Cai S, Hartwell JR, Ernstberger A, Thornton D, Brail L and Hutchins G: In vivo measurements of tumor metabolism and growth after administration of enzastaurin using small animal FDG positron-emission tomography. J Oncol *2009*: 8, 2009. PMID: 19503801. DOI: 10.1155/2009/596560

Received February 24, 2019
Revised April 10, 2019
Accepted April 15, 2019